Multirate Feedforward Control with State Trajectory Generation based on Time Axis Reversal for Plant with Continuous Time Unstable Zeros

Wataru Ohnishi[1], Hiroshi Fujimoto[1]

***Abstract*— Plant with unstable zeros is known as difficult to be controlled because of initial undershoot of step response and unstable poles of its inversion system. There are two reasons why plant has unstable zeros in discrete time domain: 1) non-collocation of actuators and sensors, 2) discretization by zero-order-hold. Problem 2) has been solved by multirate feedforward control proposed by our research group. This paper extends this method to solve problem 1) by the state trajectory generation based on time axis reversal. The validity of the proposed methods is demonstrated by simulations.**

I. Introduction

Plant with unstable zeros is known as difficult to be controlled because of unstable poles of its inversion system for a feedforward controller and initial undershoot of step response shown in Fig. 1. Zeros of the discretized transfer function can be classified as two types [1][2]: 1) intrinsic zeros, and 2) discretization zeros [3]. Intrinsic zeros correspond to zeros of its continuous time transfer function. The others are called discretization zeros.

The poles of the continuous time domain transfer function are determined by the plant dynamics such as the mass, damping, and stiffness. On the other hand, zeros of the continuous time domain are determined by not only dynamics but also the characteristics of the actuators and sensors [4]. Therefore, "integrated design of mechanism and control" is conducted to place zeros to desired position [5][6][7][8].

However, in most cases, it is difficult to change the characteristics of the actuators and sensors to allocate zeros at the desired position. For instance, zeros of wafer stages are position dependent [9] because wafer stages are need to be controlled for the lens coordinate. Other examples are hard disk drives [10], atomic force microscopes [11], bust converters [12], and interior permanent magnet synchronous motors [13].

In practice, controllers are need to be discretized for implementation. In single rate control scheme, perfect tracking [14] is not achievable because the discretization zero(s) are unstable when the plant relative order is greater than two even without intrinsic unstable zero(s). To deal with this problem, the approximate inverse based feedforward control approaches such as nonminimum-phase zeros ignore (NPZI) [15], zero-phase-error tracking controller (ZPETC) [14], and zero-magnitude-error tracking controller (ZMETC) [16] are proposed. Other approaches are FIR filter based combined input shaping and feedforward methods [17][18][19]. These methods deal with the problem 1) and 2) in the same time

[1]The University of Tokyo, 5-1-5 Kashiwanoha, Kashiwa, Chiba, 277-8561, Japan, ohnishi@hflab.k.u-tokyo.ac.jp, fujimoto@k.u-tokyo.ac.jp

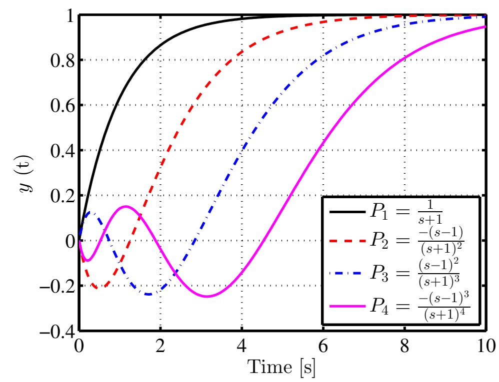

Fig. 1. Step response comparison. P_1 is 1st order transfer function without unstable zero . P_2, P_3, P_4 have one, two, three unstable zero(s) as shown in the legend of the figure. Step responses of the system with unstable zero(s) make undershoot.

because these controllers are designed by discretized transfer functions.

Unstable intrinsic and discretization zeros compensation methods by the preactuation and preview are proposed in [10][20]. These methods also compensate for intrinsic and discretization zeros in the same time. Continuous time domain approach is proposed in [21]. This method solves the differential equation in continuous time domain. In this method, however, the reference trajectory has to be defined by one equation in the positive time domain.

This paper proposes Preactuation Perfect Tracking Control method based on multirate feedforward and state trajectory generation by time axis reversal. This method solves problem 1) and 2) separately. The unstable zeros in the continuous time transfer function are managed by a state trajectory generation based on time axis reversal and preactuation commands. This method can be applied for any kind of reference position trajectory as long as $n-1$ th derivative of the trajectory is given. Here, n denotes the order of the plant in the continuous time transfer function. Next, the plant discretization problem is solved by the multirate feedforward control [22]. Finally, the relationship between the pre/post actuation and the continuous time domain unstable/stable zero(s) is clearly described. The effectiveness of the proposed method is verified by simulations.

II. Perfect Tracking Control method based on multirate feedforward (conventional)

There are two types of zeros in discretized transfer functions called intrinsic zeros and discretization zeros [1][2].

In the case of the plant with stable zeros in the continuous time domain, the intrinsic zeros are stable in the discretized domain. However, the discretized zeros are unstable when the relative degree of the continuous time plant is greater than two [3]. Because of this reason, in the single rate control scheme, the perfect tracking control (PTC) defined in [14] is impossible even without modeling error and disturbance.

In the multirate control scheme, the perfect tracking control can be achieved [22] for the plant with unstable discretized zeros. Perfect tracking control method based on multirate feedforward has been applied for high-precision stages [23][24], hard disk drives [25], atomic force microscopes [26], machining tools [27] etc. However, this method cannot be applied for the plant with continuous time domain unstable zeros without approximation because the state trajectory diverges. This problem is solved by the state trajectory generation based on time axis reversal proposed in the section III.

A. Plant definition

Nominal plant in continuous time domain is defined as a control canonical form:

$$\begin{aligned} P_c(s) &= \frac{B(s)}{A(s)} = \frac{b_m s^m + b_{m-1}s^{m-1} + \cdots + b_0}{s^n + a_{n-1}s^{n-1}\cdots + a_0} && (1)\\ \dot{\boldsymbol{x}}(t) &= \boldsymbol{A}_c\boldsymbol{x}(t) + \boldsymbol{b}_c u(t) && (2)\\ y(t) &= \boldsymbol{c}_c\boldsymbol{x}(t) && (3) \end{aligned}$$

where

$$\begin{aligned} &\boldsymbol{x} = \begin{bmatrix} x_1 \\ x_2 \\ \vdots \\ x_n \end{bmatrix}, \boldsymbol{A}_c = \begin{bmatrix} 0 & 1 & 0 & \cdots & 0 \\ 0 & 0 & 1 & \cdots & 0 \\ & & & \ddots & \\ -a_0 & -a_1 & -a_2 & \cdots & -a_{n-1} \end{bmatrix} \\ &\boldsymbol{b}_c = \begin{bmatrix} 0 & 0 & \cdots & 1 \end{bmatrix}^{\mathrm{T}} \\ &\boldsymbol{c}_c = \begin{bmatrix} b_0 & b_1 & \cdots & b_m & 0 & \cdots & 0 \end{bmatrix} \end{aligned} \tag{4}$$

$B(s)$ and $A(s)$ denotes the irreducible numerator and denominator of $P_c(s)$. n and $m(< n)$ denotes the nominal plant order and the number of the zeros, respectively. Discretized plant of (2) and (3) by zero-order-hold with sampling time T_u is defined as

$$\begin{aligned} \boldsymbol{x}[k+1] &= \boldsymbol{A}_s\boldsymbol{x}[k] + \boldsymbol{b}_s u[k] && (5)\\ y[k] &= \boldsymbol{c}_s\boldsymbol{x}[k], && (6) \end{aligned}$$

where

$$\boldsymbol{A}_s = e^{\boldsymbol{A}_c T_u},\ \ \boldsymbol{b}_s = \int_0^{T_u} e^{\boldsymbol{A}_c \tau}\boldsymbol{b}_c d\tau,\ \ \boldsymbol{c}_s = \boldsymbol{c}_c. \tag{7}$$

B. State trajectory $\boldsymbol{x}_d$ generation

According to (3), in order to track the reference position trajectory $r(t)$, the desired state trajectory $\boldsymbol{x}_d$ should satisfy

$$r(t) = \boldsymbol{c}_c\boldsymbol{x}_d(t). \tag{8}$$

In plant without continuous time zeros cases, the state trajectory $\boldsymbol{x}_d = [x_{1d}\, x_{2d}\, \cdots\, x_{nd}]^{\mathrm{T}}$ becomes $\frac{1}{b_0}[r\ sr\ \cdots\ s^{n-1}r]^{\mathrm{T}}$ considering $\boldsymbol{c}_c = [b_0\ 0\ \cdots\ 0]$ in (8). For instance, in the case of a second order rigid body plant, the state trajectory coincides the position and velocity references.

Generally, in the plant with continuous time zeros case, the state trajectory is obtained by [25]

$$\boldsymbol{x}_d(t) = \int_0^t f(t-\tau)\boldsymbol{r}(\tau)d\tau, \tag{9}$$

where

$$f(t) = \bar{\mathcal{L}}^{-1}\left[\frac{1}{B(s)}\right], \tag{10}$$

$$\begin{aligned} \boldsymbol{r}(t) &= \begin{bmatrix} r_1(t) & r_2(t) & \cdots & r_n(t) \end{bmatrix}^{\mathrm{T}} \\ &= \begin{bmatrix} 1 & s & \cdots & s^{n-1} \end{bmatrix}^{\mathrm{T}} r(t) \end{aligned}. \tag{11}$$

Here, $\bar{\mathcal{L}}$ denotes one-sided Laplace transform.

In the case of plant with continuous time unstable zeros, $\boldsymbol{x}_d(t)$ in (9) diverges because $\frac{1}{B(s)}$ is unstable. This problem is solved by the time axis reversal proposed in the section III.

C. Feedforward output u_o generation from $\boldsymbol{x}_d$

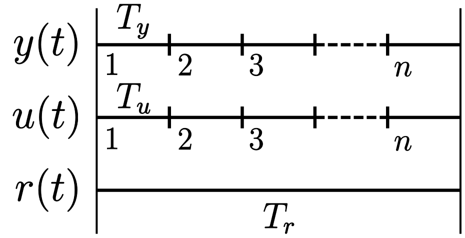

Fig. 2. Multirate sampling period.

Effect of unstable discretization zeros can be avoided by multirate feedforward control [22]. Here, as shown in Fig. 2, there are three time periods T_y, T_u, and T_r which denote the period for $y(t)$, $u(t)$, and $r(t)$. These periods are set as $T_r = nT_u = nT_y$.

The multirate system of (5) and (6) are written as

$$\boldsymbol{x}[i+1] = \boldsymbol{A}\boldsymbol{x}[i] + \boldsymbol{B}\boldsymbol{u}[i],\ \ y[i] = \boldsymbol{c}\boldsymbol{x}[i], \tag{12}$$

where

$$\begin{aligned} &\boldsymbol{A} = \boldsymbol{A}_s^n,\ \ \boldsymbol{B} = \begin{bmatrix} \boldsymbol{A}_s^{n-1}\boldsymbol{b}_s & \boldsymbol{A}_s^{n-2}\boldsymbol{b}_s & \cdots & \boldsymbol{A}_s\boldsymbol{b}_s & \boldsymbol{b}_s \end{bmatrix} \\ &\boldsymbol{c} = \boldsymbol{c}_s,\ \ \boldsymbol{x}[i] = \boldsymbol{x}(iT_r) \end{aligned} \tag{13}$$

by calculating the state transition from $t = iT_r = kT_u$ to $t = (i+1)T_r = (k+n)T_u$. Here, the input vector $\boldsymbol{u}[i]$ is defined in the lifting form:

$$\begin{aligned} \boldsymbol{u}[i] &= \begin{bmatrix} u_1[i] & u_2[i] & \cdots & u_n[i] \end{bmatrix}^{\mathrm{T}} \\ &= \begin{bmatrix} u(kT_u) & u((k+1)T_u) & \cdots & u((k+n-1)T_u) \end{bmatrix}^{\mathrm{T}} \end{aligned} \tag{14}$$

According to (12), the feedforward output $\boldsymbol{u}_o[i]$ is obtained from the previewed state trajectory $\boldsymbol{x}_d[i+1]$ as following

$$\boldsymbol{u}_o[i] = \boldsymbol{B}^{-1}(\boldsymbol{I} - z^{-1}\boldsymbol{A})\boldsymbol{x}_d[i+1], \tag{15}$$

where z denotes e^{sT_r}.

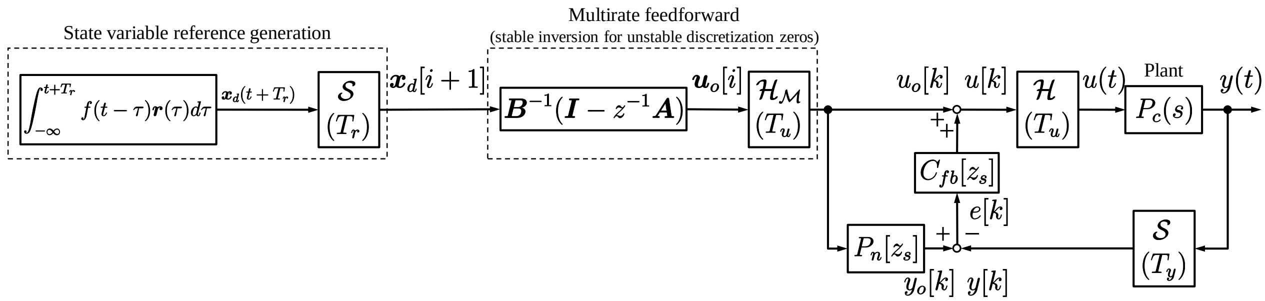

Fig. 3. Perfect Tracking Control method based on multirate feedforward proposed in reference [22]. $\mathcal{S}$, $\mathcal{H}$, $\mathcal{H}_{\mathcal{M}}$ denote a sampler, a holder, and a multirate holder, respectively. z and z_s denote e^{sT_r} and e^{sT_u}, respectively.

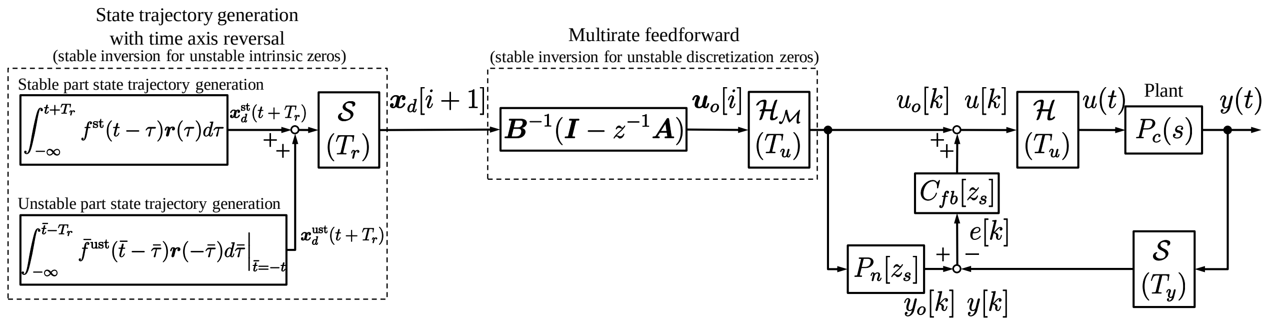

Fig. 4. Proposed Preactuation Perfect Tracking Control method based on multirate feedforward and state trajectory generation by time axis reversal.

III. Preactuation Perfect Tracking Control method based on multirate feedforward (proposed)

A. Design steps

In the case of plant with continuous time unstable zeros, the state trajectory diverges according to (9). In this section, a stable variable reference generation method for the plant with continuous time domain is formulated.

1) Separation to a stable and unstable part:

$$B(s)^{-1} = F^{\text{st}}(s) + F^{\text{ust}}(s) \tag{16}$$

$$f^{\text{st}}(t) = \bar{\mathcal{L}}^{-1}\left[F^{\text{st}}(s)\right], \bar{f}^{\text{ust}}(t) = \bar{\mathcal{L}}^{-1}\left[(-1)^l F^{\text{ust}}(-s)\right] \tag{17}$$

where $F^{\text{st}}(s)$ and $F^{\text{ust}}(s)$ have the stable and unstable pole(s), respectively. l denotes the order of $F^{\text{ust}}(s)$. Note that $F^{\text{ust}}(-s)$ is stable.

2) Stable part state trajectory generation: As for the stable part, the desired state trajectory $\boldsymbol{x}_d^{\text{st}}(t)$ is generated forwardly.

$$\begin{aligned} \boldsymbol{x}_d^{\text{st}}(t) &= \begin{bmatrix} x_{1d}^{\text{st}}(t) & x_{2d}^{\text{st}}(t) & \cdots & x_{nd}^{\text{st}}(t) \end{bmatrix}^{\text{T}} \\ &= \int_{-\infty}^{t} f^{\text{st}}(t-\tau)\boldsymbol{r}(\tau)d\tau \end{aligned} \tag{18}$$

3) Unstable part state trajectory generation: As for the unstable part, the desired state trajectory $\boldsymbol{x}_d^{\text{ust}}(t)$ is generated by

$$\begin{aligned} \boldsymbol{x}_d^{\text{ust}}(t) &= \begin{bmatrix} x_{1d}^{\text{ust}}(t) & x_{2d}^{\text{ust}}(t) & \cdots & x_{nd}^{\text{ust}}(t) \end{bmatrix}^{\text{T}} \\ &= \int_{-\infty}^{\bar{t}} \bar{f}^{\text{ust}}(\bar{t}-\bar{\tau})\boldsymbol{r}(-\bar{\tau})d\bar{\tau}\Big|_{\bar{t}=-t} \end{aligned} \tag{19}$$

$\boldsymbol{x}_d^{\text{ust}}(t)$ is calculated by two steps. First, a convolution of the time reversed reference position trajectory $\boldsymbol{r}(-\bar{t})$ and the stable signal $\bar{f}^{\text{ust}}(\bar{t})$ is calculated. Second, time axis is reversed. This method is based on the two-sided Laplace transform [28][29].

4) State trajectory generation:

$$\boldsymbol{x}_d(t) = \boldsymbol{x}_d^{\text{st}}(t) + \boldsymbol{x}_d^{\text{ust}}(t) \tag{20}$$

5) Multirate feedforward:

$$\boldsymbol{u}_o[i] = \boldsymbol{B}^{-1}(\boldsymbol{I} - z^{-1}\boldsymbol{A})\boldsymbol{x}_d[i+1] \tag{21}$$

B. Preactuation and postactuation

The proposed method shown in the section III-A clearly shows the relationship between the pre/post actuation and the continuous time domain unstable/stable zero(s). The stable zeros in the continuous time domain result in postactuation according to (18). In contrast, the unstable zeros in the continuous time domain result in the preactuation according to (19).

On the other hand, the discretization zeros are compensated by the multirate feedforward with preview formulated in (21).

IV. Simulation results

A. Simulation condition

In this section, simulations are performed by the model illustrated in Fig. 5(b). This model assumes a high-precision stage shown in Fig. 5(a) with a current feedback. Here, the continuous time domain transfer function from the current

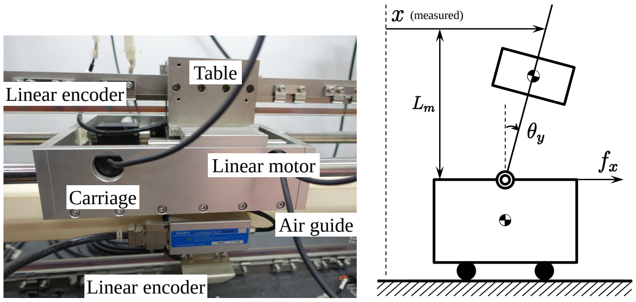

(a) High-precision stage. (b) Model of (a).

Fig. 5. Experimental high-precision stage and its model for simulation[24], [6], [30].

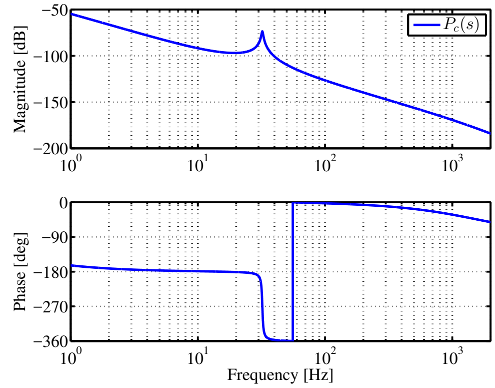

Fig. 6. Bode diagram of $P_c(s)$.

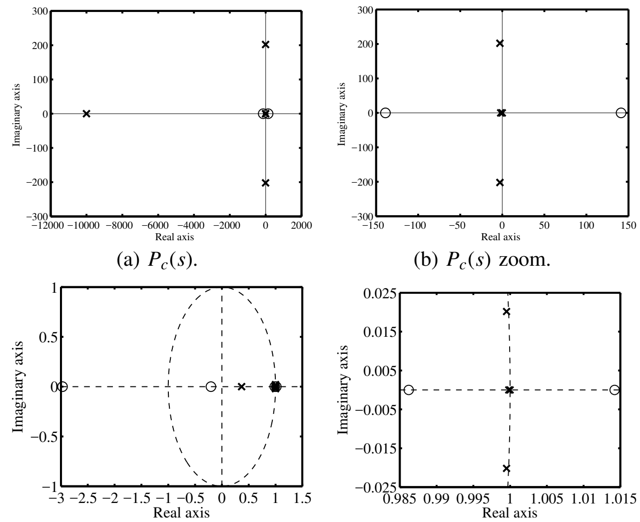

(a) $P_c(s)$. (b) $P_c(s)$ zoom.

(c) $P_s[z_s]$. (d) $P_s[z_s]$ zoom.

Fig. 7. Pole-zero map of $P_c(s)$ and $P_s[z_s]$.

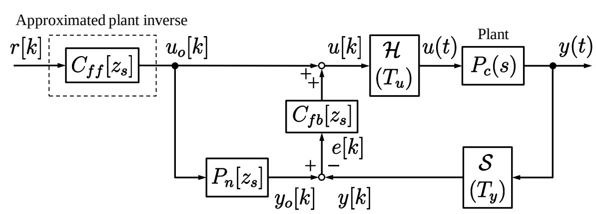

Fig. 8. Approximated plant inverse feedforward control configuration. Simulation block diagram for NPZI, ZMETC, ZPETC methods.

reference of x axis actuator which generates force f_x to the measured stage position x is defined as

$$P_c(s) = 3.048 \times 10^{10} \frac{(0.1228 - L_m)s^2 + 0.4102s + 3476}{s(s + 10000)(s + 1.846)(s^2 + 5.623s + 4.078 \times 10^4)}, \quad (22)$$

where L_m denotes the height of the measurement point illustrated in Fig. 5(b). From (22), in the case of $0.1228 < L_m$, $P_c(s)$ has a continuous time unstable zero. In this paper, $L_m = 0.300$ is considered:

$$P_c(s) = \frac{-1599(s - 141.2)(s + 138.9)}{s(s + 10000)(s + 1.846)(s^2 + 5.623s + 4.078 \times 10^4)} \quad (23)$$

Discretized transfer function of (23) by zero-order-hold with $100\,\mu$s sampling is obtained as

$$P_s[z_s] = \frac{-2.112 \times 10^{-10}(z_s + 2.971)(z_s - 1.014)(z_s - 0.9862)(z_s + 0.2045)}{(z_s - 1)(z_s - 0.9998)(z_s - 0.3679)(z_s^2 - 1.999z_s + 0.9994)}, \quad (24)$$

where z_s denotes e^{sT_u}. Bode diagram of $P_c(s)$ and pole-zero map of $P_c(s)$ and $P_s[z_s]$ are shown in Fig. 6 and 7. In the continuous time domain, $P_c(s)$ has one stable zero ($s = -138.9$) and one unstable zero ($s = +141.2$). In the discrete time domain, $P_s[z_s]$ has the intrinsic zeros at $z_s = +1.014$ and the discretized zeros at $z_s = -2.971, -0.2045$. Here, $P_s[z_s]$ has one unstable intrinsic zero and one unstable discretized zero.

Step target trajectory $r(t)$ is designed as Fig. 10(a) by 9th order polynomial during step motion. Step time is set as 0.02 [s]. In Fig. 4 and 8 configurations, the feedback controller $C_{fb}[z_s]$ generates force only if modeling error or disturbance exist. Simulation step is set as $1\,\mu$s. Simulations are conducted between -1.0 [s] $< t < 1.0$ [s].

B. Simulation results of the proposed method

Simulation results are shown in Fig. 9 and 10. The reference position trajectory $\boldsymbol{r}(t)$ and the generated state trajectory $\boldsymbol{x}_d(t), \boldsymbol{x}_d^{\mathrm{st}}(t), \boldsymbol{x}_d^{\mathrm{ust}}(t)$ are shown in Fig. 9. The continuous time domain unstable zero generates the state trajectory in the negative time domain by (18).

Fig. 10(a) and 10(c) indicate that the output trajectory $y(t)$ can track the reference position trajectory $r(t)$ without any undershoot or overshoot. Fig. 10(c) demonstrates the perfect tracking is achieved for every $T_r = 500\,\mu$s by the proposed method. Fig. 10(e) shows the preactuation ($t < 0$) and postactuation ($0.02 < t$). Fig. 9 and Fig. 10(e) indicate that the preactuation and postactuation are caused by the $\boldsymbol{x}_d^{\mathrm{ust}}(t)$ and $\boldsymbol{x}_d^{\mathrm{st}}(t)$, respectively. Note that the unstable discretization zero ($z_s = -2.971$) is compensated by the multirate feedforward scheme introduced in the section II.

From the above, the effectiveness of the proposed Preactuation Perfect Tracking Control method based on multirate feedforward and state trajectory is verified.

C. Comparison of approximated inverse methods

Simulation results of the NPZI method [15], the ZPETC method [14], and the ZMETC method [16] are also shown in Fig. 10. Block diagram shown in Fig. 8 is used for these methods. These three methods are designed by sampling

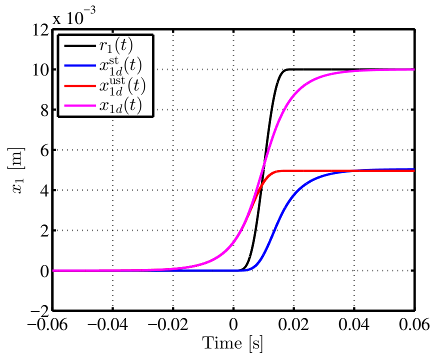

(a) $r_1(t), x_{1d}^{st}(t), x_{1d}^{ust}(t), x_{1d}(t)$.

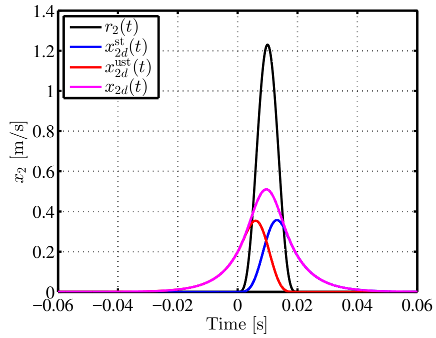

(b) $r_2(t), x_{2d}^{st}(t), x_{2d}^{ust}(t), x_{2d}(t)$.

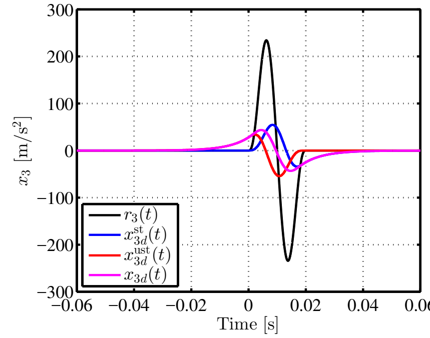

(c) $r_3(t), x_{3d}^{st}(t), x_{3d}^{ust}(t), x_{3d}(t)$.

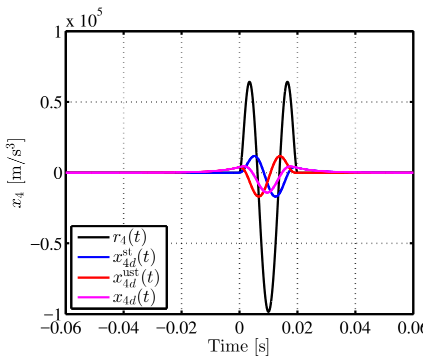

(d) $r_4(t), x_{4d}^{st}(t), x_{4d}^{ust}(t), x_{4d}(t)$.

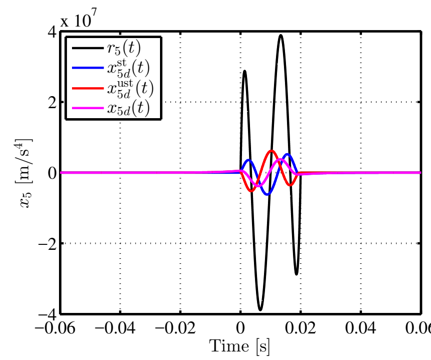

(e) $r_5(t), x_{5d}^{st}(t), x_{5d}^{ust}(t), x_{5d}(t)$.

Fig. 9. Generated state trajectory by time axis reversal (see equations (18), (19), and (20)).

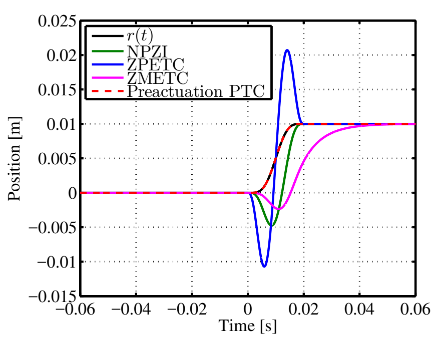

(a) Position.

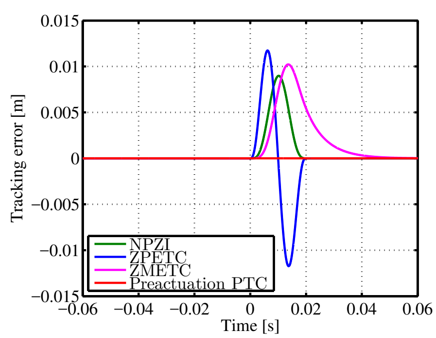

(b) Tracking error.

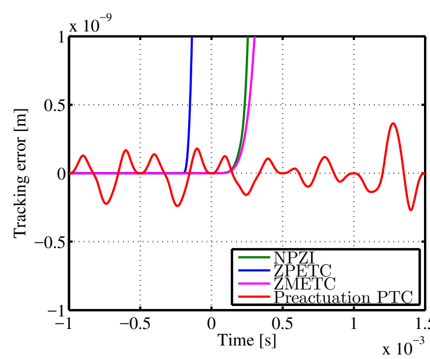

(c) Tracking error (zoom).

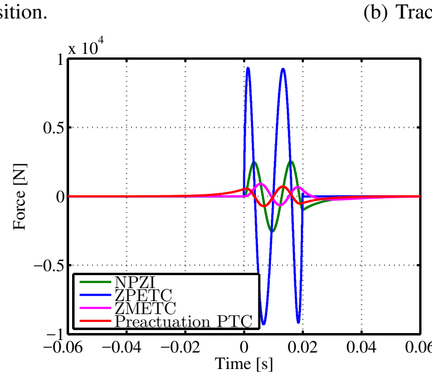

(d) Force.

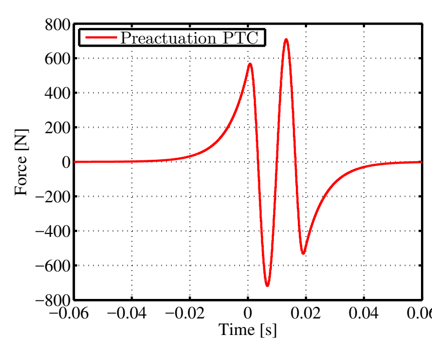

(e) Force (Preactuation PTC).

Fig. 10. Simulation results of the plant with continuous time unstable zero. From (c), the perfect tracking is achieved for every $T_r = 500\,\mu$s.

period T_u. In the ZPETC, preview is used to achieve the zero phase error characteristics.

These methods create the undershoot and/or overshoot to compensate for the unstable intrinsic zero ($z_s = +1.014$) and the unstable discretization zero ($z_s = -2.971$). From the above, without the preactuation, there are trade-offs between the undershoot and/or overshoot amplitude and settling time.

V. Conclusion

This paper proposes the Preactuation Perfect Tracking Control method based on multirate feedforward and state trajectory generation by time axis reversal. In the discretized domain, there are two types of zeros: 1) the intrinsic zeros which have counterparts in the continuous time domain, 2) the discretization zeros generated by discretization. In the non-collocated system, the discretized plant has unstable intrinsic zeros. On the other hand, the discretized zeros become unstable when the relative degree of the plant in the continuous time domain is greater than two.

Proposed method deals with problem 1) and 2) separately. The unstable intrinsic zeros are compensated by the preactuation. The reference of the preactuation is generated by the negative time domain state trajectory calculated by the time axis reversal procedure. Next, the unstable discretization zeros are compensated by the multirate feedforward scheme with preview. The effectiveness of proposed method is demonstrated by simulations. Comparison with other preview/preactuation based methods will be performed.

Acknowledgment

This work is supported by JSPS KAKENHI Grant Number 15J08488.

References

[1] T. Hagiwara, T. Yuasa, and M. Araki, "Stability of the limiting zeros of sampled-data systems with zero-and first-order holds," *International Journal of Control*, vol. 58, no. 6, pp. 1325–1346, 1993.

[2] T. Hagiwara, "Analytic study on the intrinsic zeros of sampled-data systems," *IEEE Transactions on Automatic Control*, vol. 41, no. 2, pp. 261–263, 1996.

[3] K. Åström, P. Hagander, and J. Sternby, "Zeros of sampled systems," *Automatica*, vol. 20, no. 1, pp. 31–38, 1984.

[4] J. Hoagg and D. Bernstein, "Nonminimum-phase zeros - much to do about nothing - classical control - revisited part II," *IEEE Control Systems*, vol. 27, no. 3, pp. 45–57, 2007.

[5] T. Atsumi, T. Arisaka, T. Shimizu, and T. Yamaguchi, "Vibration Servo Control Design for Mechanical Resonant Modes of a Hard-Disk-Drive Actuator," *JSME International Journal Series C*, vol. 46, no. 3, pp. 819–827, 2003.

[6] A. Hara, K. Saiki, K. Sakata, and H. Fujimoto, "Basic examination on simultaneous optimization of mechanism and control for high precision single axis stage and experimental verification," in *34th Annual Conference of IEEE Industrial Electronics*, pp. 2509–2514, 2008.

[7] W. Ohnishi, H. Fujimoto, K. Sakata, K. Suzuki, and K. Saiki, "Integrated Design of Mechanism and Control for High-Precision Stages by the Interaction Index in the Direct Nyquist Array Method," in *American Control Conference*, pp. 2825–2830, 2015.

[8] W. Ohnishi, H. Fujimoto, K. Sakata, K. Suzuki, and K. Saiki, "Decoupling Control Method for High-Precision Stages using Multiple Actuators considering the Misalignment among the Actuation Point, Center of Gravity, and Center of Rotation," *IEEJ Journal of Industry Applications*, vol. 5, no. 2, pp. 141–147, 2016.

[9] H. Butler, "Position Control in Lithographic Equipment," *IEEE Control Systems Magazine*, vol. 31, no. 5, pp. 28–47, 2011.

[10] B. Rigney, L. Y. Pao, and D. Lawrence, "Nonminimum phase dynamic inversion for settle time applications," *IEEE Transactions on Control Systems Technology*, vol. 17, no. 5, pp. 989–1005, 2009.

[11] L. Y. Pao, J. A. Butterworth, and D. Y. Abramovitch, "Combined feedforward/feedback control of atomic force microscopes," in *American Control Conference*, pp. 3509–3515, 2007.

[12] Z. Chen, W. Gao, J. Hu, and X. Ye, "Closed-loop analysis and cascade control of a nonminimum phase boost converter," *IEEE Transactions on Power Electronics*, vol. 26, no. 4, pp. 1237–1252, 2011.

[13] T. Miyajima, H. Fujimoto, and M. Fujitsuna, "A Precise Model-Based Design of Voltage Phase Controller for IPMSM," *IEEE Transactions on Power Electronics*, vol. 28, no. 12, pp. 5655–5664, 2013.

[14] M. Tomizuka, "Zero phase error tracking algorithm for digital control," *Journal of Dynamic Systems, Measurement, and Control*, vol. 109, pp. 65–68, 1987.

[15] J. A. Butterworth, L. Y. Pao, and D. Y. Abramovitch, "Analysis and comparison of three discrete-time feedforward model-inverse control techniques for nonminimum-phase systems," *Mechatronics*, vol. 22, no. 5, pp. 577–587, 2012.

[16] J. Wen and B. Potsaid, "An experimental study of a high performance motion control system," in *American Control Conference*, vol. 6, pp. 5158–5163, 2004.

[17] D. Bruijnen and N. van Dijk, "Combined input shaping and feedforward control for flexible motion systems," in *American Control Conference*, pp. 2473–2478, 2012.

[18] M. Heertjes and D. Bruijnen, "MIMO FIR Feedforward Design for Zero Error Tracking Control," in *American Control Conference*, pp. 2166–2171, 2014.

[19] M. O. Navarrete, M. F. Heertjes, and R. H. M. Schmidt, "Common Zeros in Synchronization of High-Precision Stage Systems," in *IEEE International Conference on Mechatronics*, pp. 598–603, 2015.

[20] L. Marconi, G. Marro, and C. Melchiorri, "A solution technique for almost perfect tracking of non-minimum-phase, discrete-time linear systems," *International Journal of Control*, vol. 74, no. 5, pp. 496–506, 2001.

[21] T. Shiraishi and H. Fujimoto, "A Reference Trajectory Generation for System with Unstable Zeros Considering Negative-time Domain Analysis," in *IEEJ International Workshop on Sensing, Actuation, and Motion Control*, 2015.

[22] H. Fujimoto, Y. Hori, and A. Kawamura, "Perfect tracking control based on multirate feedforward control with generalized sampling periods," *IEEE Transactions on Industrial Electronics*, vol. 48, no. 3, pp. 636–644, 2001.

[23] K. Saiki, A. Hara, K. Sakata, and H. Fujimoto, "A Study on High-Speed and High-Precision Tracking Control of Large-Scale Stage Using Perfect Tracking Control Method Based on Multirate Feedforward Control," *IEEE Transactions on Industrial Electronics*, vol. 57, no. 4, pp. 1393–1400, 2010.

[24] H. Fujimoto, K. Sakata, and K. Saiki, "Application of Perfect Tracking Control to Large-Scale High-Precision Stage," in *5th IFAC Symposium on Mechatronic Systems*, pp. 188–193, 2010.

[25] H. Fujimoto, K. Fukushima, and S. Nakagawa, "Vibration suppression short-span seeking of HDD with multirate feedforward control," in *American Control Conference*, pp. 582–587, 2006.

[26] T. Shiraishi and H. Fujimoto, "Positioning control for Piezo scanner using multirate perfect inverse model based iterative learning control," in *IEEE/ASME International Conference on Advanced Intelligent Mechatronics*, pp. 993–998, 2010.

[27] H. Fujimoto and T. Takemura, "High-precision control of ball-screw-driven stage based on repetitive control using n-times learning filter," *IEEE Transactions on Industrial Electronics*, vol. 61, no. 7, pp. 3694–3703, 2014.

[28] T. Sogo, "Calculation of the Non-causal Solution for the Model-matching Problem and Its Application to Preview Feedforward Control," *Transactions of the Society of Instrument and Control Engineers*, vol. 42, no. 1, pp. 40–46, 2006. (in Japanese)

[29] T. Sogo, "An algebraic expression of stable inversion for nonminimum phase systems and its applications," in *the 17th IFAC world congress*, vol. 17, pp. 2820–2825, 2008.

[30] T. Shiraishi and H. Fujimoto, "Trajectory tracking control method based on zero-phase minimum-phase factorization for nonminimum-phase continuous-time system," in *International Workshop on Advanced Motion Control*, pp. 1–6, 2012.